Deposition of titanium dioxide particles on kanthal coils by direct heating technique for photodegradation of methylene blue solution

Guan Sheng Ng[1], Chee Meng Koe[1] and Swee-Yong Pung[*]

School of Materials and Mineral Resources Engineering, Engineering Campus, Universiti Sains Malaysia, 14300 Nibong Tebal, Pulau Pinang, Malaysia

ABSTRACT

Organic dyes are extensively used in textile and batik industry. Dispose of untreated dye effluent into water system is hazardous to human and environment. Advanced oxidation process (AOPs) based on heterogeneous TiO_2 photocatalyst is proven for effluent treatment. Immobilization of TiO_2 photocatalyst on supporting substrate is one of the research focuses to realize its application in industry to minimize the loss of TiO_2 photocatalyst over time during effluent treatment. Many synthesis techniques have been used to grow TiO_2 photocatalyst on supporting substrates. However, these synthesis techniques are either time- or cost-consuming. In this work, a novel direct heating (DH) technique has been developed for the first time to deposit TiO_2 particles on kanthal coils. The optimum deposition of TiO_2 particles was achieved in 15 min using 60 W. The TiO_2 particles contained mixture of anatase (82.7%) and brookite (17.3%), with an average particle size of 167.36±15.37 nm. The surface coverage of TiO_2 particles on kanthal wire was good, with minimum agglomeration. The TiO_2 particles deposited on kanthal coils recorded 43.7% of photodegradation efficiency in methylene blue removal under UV light.

1. INTRODUCTION

In order to maintain a healthy ecosystem, high quality surface water and safe drinking water is an essential. Water pollution by human had make the water unsafe for human use and disrupts the aquatic ecosystems. Nowadays, water pollution is the major problem in the global context. The conventional priority pollutants could be found in wastewater are countless, including organic dyes [1], pesticides [2], lead [3], arsenic [4], polychlorinated biphenyls (PCBs) [5] and poly aromatic hydrocarbons (PAHs) [6].

Organic dyes are one of the most serious pollutants in the world. Dyes are extensively used in numerous industries for examples in textile, batik, rubber, paper, food and plastics. The effluents from these industries are in coloured form. Discharge of untreated waste into the water systems will lead to severe pollution to the aquatic life and environment. Among all the industries, textile industry is one of the largest producers of the liquid effluent pollutants as huge amount of water is needed in the dyeing process [1].

Methylene Blue (MB), is one types of synthetic dyes [7], that soluble in water. It can form quaternary ammonium cations in aqueous solution, and it also has a high chroma which can cause serious environmental pollution. The major sources of MB dye effluents to the environment are from pharmaceutical industries, textile industries, paints and varnishing industries, food industries, and leather industries. Besides, the minor sources of dye effluents are wastewater treatment plant and household. During the sewage treatment, the dyes are usually not

---

[*] Corresponding author: sypung@usm.my

quantitatively removes as they can escape the degradation in waste treatment plants and remain in the effluents that are able to get into the surface and groundwater [8].

Common wastewater treatment plants are difficult and non-economical to completely remove this kind of organic dye pollutants (e.g., MB) particularly in low concentration (ppm level). These azo and reactive dyes are electron-deficient in nature, which makes them less susceptible to oxidative catabolism. Moreover, the MB dye presents in wastewater has high stability, complex composition, anti-biodegradable properties which make it difficult to be degraded. The MB residuals could be intake by human and animals through tap water and other water sources, causing various health issues.

AOPs is generally a degradation technology that uses the hydroxyl radicals which is the ultimate oxidant to degrade organic contaminants in wastewater [9]. AOP based on semiconductor photocatalysts is a complementary technique to degrade the non-biodegradable and highly stable organic compounds. The presence of the catalyst will accelerate the AOPs due to the presence of electron-hole pairs. The photogenerated electrons and holes produced free radicals that result in effective oxidation and reduction processes on the organic pollutants [10]. The organic pollutants will breakdown into smaller molecules such as water and carbon dioxide at the end of photocatalytic process.

TiO_2 is a widely used photocatalyst for organic dyes removal [11, 12]. The use of TiO_2 photocatalyst in particle form is not suitable as it tends to drain away by wastewater. Thus, efforts have been done to deposit TiO_2 photocatalyst on supporting substrates to reduce the loss of TiO_2 photocatalyst over time during effluent treatment. There are various synthesis techniques that can be used to synthesize TiO_2 particles such as hydrothermal method [13], template-assisted method [14], sol-gel method [15], electrochemical anodizing method [16], microwave-assisted method [17], and chemical vapour deposition method [18]. However, the major problems of these methods are either required high equipment cost, consumed high electrical power, or taken long synthesis duration. For instances, Sun et al. took 36 hrs to produce TiO_2 nanotubes using hydrothermal technique [13], whereas Qiang Zhang et al. synthesized TiO_2 films at 300 °C to 400 °C using chemical vapour deposition techniques [18]. In these synthesis techniques, heat is generated outside the reactor before transferring into the reactor for the growth of TiO_2 photocatalyst. A lot of heat is wasted to surrounding. Consequently, the synthesis process takes long synthesis duration (in hours) and consume a lot of electrical power (in kW.h).

DH technique is a simple one step process. In this work, the electrical current was introduced directly to the kanthal coils, allowing rapid heating of the substrate for the deposition of TiO_2 photocatalyst. As minimum heat was loss to surrounding, it used less than 60 W.h and less than 1 hour for the whole synthesis process. Our previous work has demonstrated synthesis of TiO_2 particles by DH technique [19]. The focus of this work is to immobilize TiO_2 particles on the supporting substrate (kanthal coils) by DH technique instead. Additionally, the efficiency of the novel fabricated catalyst on the photodegradation of MB dye using UV light and the reaction kinetics were studied.

2. RESEARCH METHODOLOGY

2.1 Deposition of TiO_2 particles on kanthal coils by DH technique

A 30 cm length of kanthal wire (FeCrAl, diameter: 0.812 mm) was cut from the wire spool by wire cutter. It was winded around a pen to produce a wire coil with 8 turns without overlapping. The coil was 20 mm in length as shown in **Figure 1(a)**. The kanthal coil was degreased and cleaned in acetone bath for 15 minutes under sonification. This was followed by cleaning in isopropanol

bath for 15 minutes under sonification. Lastly, the coil was cleaned in deionised water bath for another 10 minutes and left for air dried.

(a)

(b)
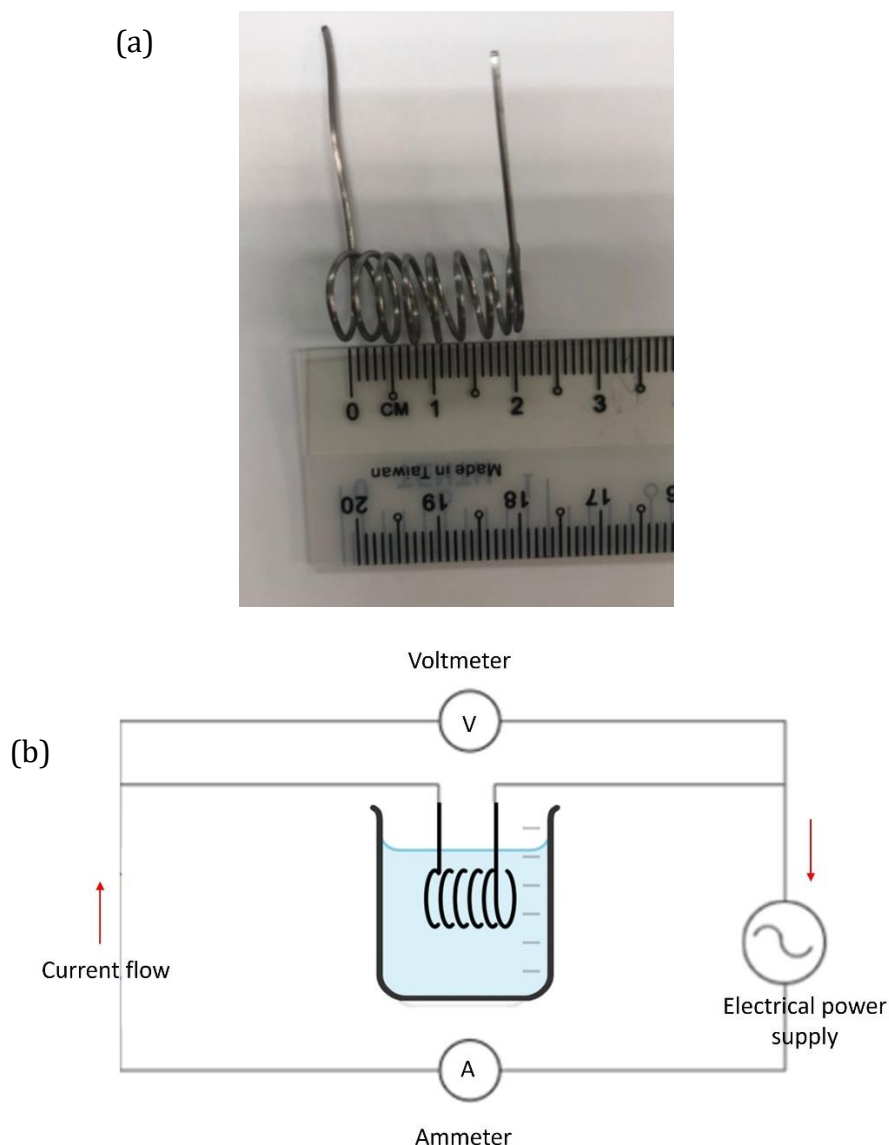
Figure 1. (a) Kanthal wire (substrate material) with 8 turns and 20 mm in length, and (b) Schematic diagram of setup of DH technique.

Figure 1 (b) shows the setup of DH technique. The precursor solution was prepared by mixing 5 ml of titanium tetraisopropoxide (TTIP) (Sigma Aldrich) with 15 ml isopropanol (Sigma Aldrich). A 250 ml solution of distilled water was mixed with hydrochloric acid solution (HCl) (QReC) to reach pH 1. Then, 2 drops of oxidizing agent, i.e., hydrogen peroxide (H_2O_2) (Merck) were added to the mixture solution to promote the formation of TiO_2. Subsequently, the TTIP mixture solution was hydrolysed by adding dropwise into the acid solution under constant stirring using magnetic stirrer. The kanthal coil was immersed into the precursor solution. The electrical power supply was switched on and the applied electric power was adjusted to 60 W. The effect of heating duration on the deposition of TiO_2 particles on the surface kanthal wires was studied. The heating duration was varied from 0 (bare kanthal wire), 15, 30, 45 and 60 min. At the end of synthesis process, the kanthal coils were rinsed with distilled water and air dried prior to characterizations.

The crystal phases of deposits were characterized using X-ray diffractometer (XRD Bruker D2 Phaser). The XRD target was copper, emitting X-ray with 0.15406 nm wavelength (Cu K$_\alpha$). The quantity of deposit found on the surface of kanthal coils was small. In addition, the bending of kanthal coils made it difficult to be analyzed by XRD. Therefore, the deposits were collected by sonicating the kanthal coils for 15 min. The deposits were dried prior sending for XRD analysis. The scanning range of XRD analysis was performed from 10º to 90º of 2θ at accelerating voltage of 30 kV. The XRD data was analyzed by X'pert Highscore Plus software. The morphology of deposit was characterized using scanning electron microscope (FEI Quanta 650 FEG Scanning Electron Microscope). The size of the particles that deposited on kanthal wire was subsequently measured by Image J software. The UV-visible spectrometer (Varian Cary 50) was used to measure the characteristic absorbance of degraded MB solution at 664 nm.

2.2   Photocatalytic degradation of methylene blue solution by TiO$_2$ particles

The photocatalytic activity of the TiO$_2$ particles deposited on kanthal coils was studied. A 100 ml of MB solution (1 mg L^{-1}) and TiO$_2$ deposited coils were kept in a beaker. The solution was stirred in the dark room for 30 minutes to establish an adsorption-desorption equilibrium between the MB solution and the surface of TiO$_2$ particles. Then, UV light (λ = 254 nm) was switched on to trigger the photocatalytic process. All the experiments were conducted at room temperature. A 4.5 mL of aliquots were sampled at every 15 minutes intervals until 90 minutes. The absorbance of the samples collected at different time interval were measured by UV-Vis spectroscopy. According to Beer-Lambert rule, the absorbance of solution is proportional to its concentration. Therefore, the photodegradation efficiency of TiO$_2$ particles deposited on kanthal coils in removal of MB could be calculated using Equation 1:

$$\text{Photodegradation efficiency (\%)} = \frac{C_0 - C_t}{C_0} \times 100 \tag{1}$$

where C_o is the initial MB concentration in the solution, C_t is the residual MB concentration after the irradiation time (t) respectively.

Besides, the kinetic reaction of MB dye by TiO$_2$ particles deposited on kanthal coils were studied by plotting various graphs followed the formula for pseudo-zero-order, pseudo-first-order, and pseudo-second-order kinetic models as shown in Equation 2, 3 and 4.

$$\text{Pseudo-zero-order: } C_t = k_0 t + C_o \tag{2}$$

$$\text{Pseudo-first-order: } \ln\left(\frac{C_o}{C_t}\right) = k_1 t \tag{3}$$

$$\text{Pseudo-second-order: } \frac{1}{C_t} = \frac{1}{C_o} + k_2 t \tag{4}$$

where C_o is the initial MB concentration in the solution, C_t is the residual MB concentration after the irradiation time (t), and k_0, k_1, k_2 is the zero-order, first-order, and second-order rate constants, respectively.

3.   RESULTS AND DISCUSSION

3.1   Appearance of kanthal coil before and after DH process

Figure 2 shows the kanthal coil before and after Direct Heating process. The synthesis process was carried out using 15 minutes of heating duration and heating power of 60 W. As compared to bare kanthal coil (left, shiny surface), a white layer of deposit was found on the surface kanthal coil after the synthesis process. Systematic research was performed by studying the effects of

heating duration and heating power on the growth of these deposits and their photocatalytic performances in MB removal.
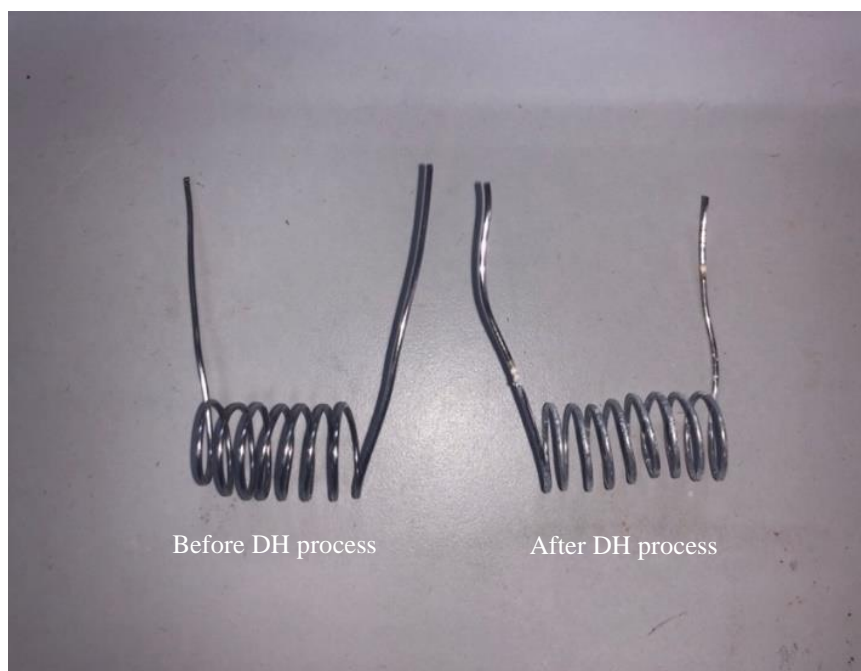
Figure 2. Appearance of kanthal coil (a) before and (b) after the DH process.

3.2 Effect of heating duration

The effect of heating duration on the deposition of TiO_2 particles on kanthal coils was studied. **Figure 3** shows the XRD patterns of particles produced at various heating durations. The diffraction peaks at the positions of 2θ = 25.28°, 37.60°, 48.00°, 53.92°, 69.00° could be indexed to the (101), (004), (200), (105), (116) of tetragonal anatase phase TiO_2 (ICSD 98-005-9309). It is noted that the anatase TiO_2 was found in all the particles produced by DH. Besides, the diffraction peaks at the positions of 2θ = 30.80°, 63.00° corresponds to Miller indices of (121), (601) of an orthorhombic brookite TiO_2 (ICSD 98-010-5395). During the formation of TiO_2 particles, anatase phase crystallite is known to be formed prior to other phases [20]. The (112) anatase twin interfaces contain a unit cell of brookite. Brookite was able to nucleate at these twin planes and grow at the expense of anatase at low temperature (reacting temperature at this work was in the range of 30 °C–90 °C) [21]. Therefore, anatase and brookite phases were observed. Rietveld refinement method was used to estimate the amount of crystal phases that produced by DH technique. As displayed in **Table 1**, the main crystal phase of TiO_2 particles produced at different synthesis duration was anatase (>71.4 %). Brookite TiO_2 was the secondary crystal phase, varying in the range of 5.0 – 28.6%.

Figure 4 shows the surface of kanthal coils produced at different heating durations observed under low magnification (500X). The bare kanthal coil has relatively smooth surface as shown in **Figure 4(a)**. Grooves induced parallelly due to the extrusion process during fabrication of kanthal wire are clearly seen as highlighted in the arrows. The TiO_2 deposits could be seen on the surface of kanthal coils. The TiO_2 deposits was uneven and randomly found on the surface of kanthal coils. It is found that the surface coverage of TiO_2 deposits increased with increasing heating duration. The TiO_2 layer started forming at 15 min of heating duration and covered the grooves as shown in **Figure 4(b)**. In fact, a thick layer of TiO_2 was formed on the surface of kanthal coils at pro-long synthesis durations (60 min), covering the grooves of kanthal coils.

Figure 5 shows the morphology of deposits at high magnification (30 kX). No deposition was found on the smooth surface of bare kanthal coil (0 min) as shown in **Figure 5(a)**. The TiO_2 particles were deposited on the surface of Kanthal wires at all heating durations when the electrical power was turned on. The amount of TiO_2 particles increased with synthesis duration. These TiO_2 particles tended to agglomerate and form thick TiO_2 layer as seen in **Figure 5(e)**. The agglomeration of TiO_2 particles was due to the adhesion of particles to each other by weak forces lead to (sub) micron size of TiO_2 particles [22]. Moreover, small particles having high surface area tended to stabilize themselves either by adsorption of molecules from the surrounding or by lowering the surface area through agglomeration.
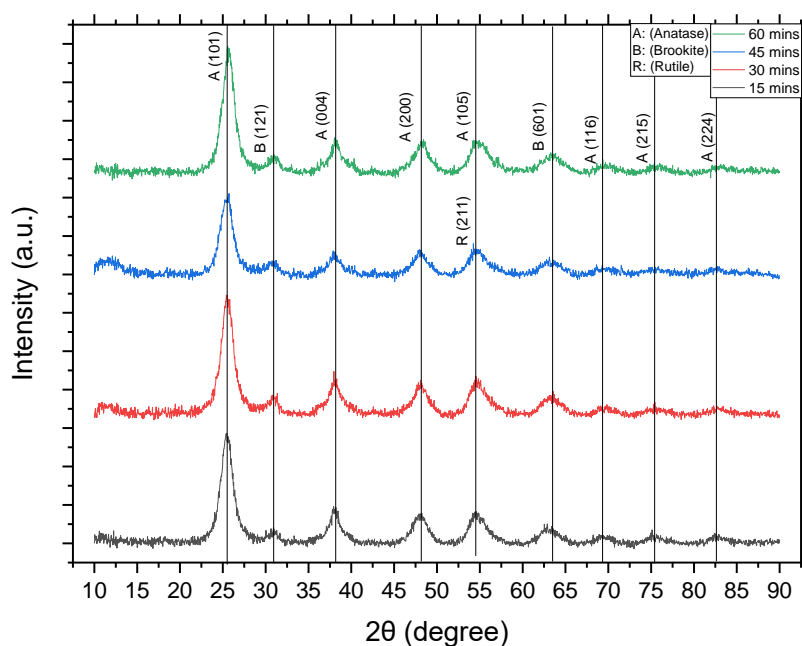
Figure 3. XRD patterns of TiO_2 particles produced at different heating duration using DH technique

Table 1 The amount of TiO_2 crystal phases produced at different heating duration using DH technique

Heating Duration (min)	Phase content (wt. %)	
	Anatase	Brookite
15	82.7	17.3
30	89.0	11.0
45	95.0	5.0
60	71.4	28.6
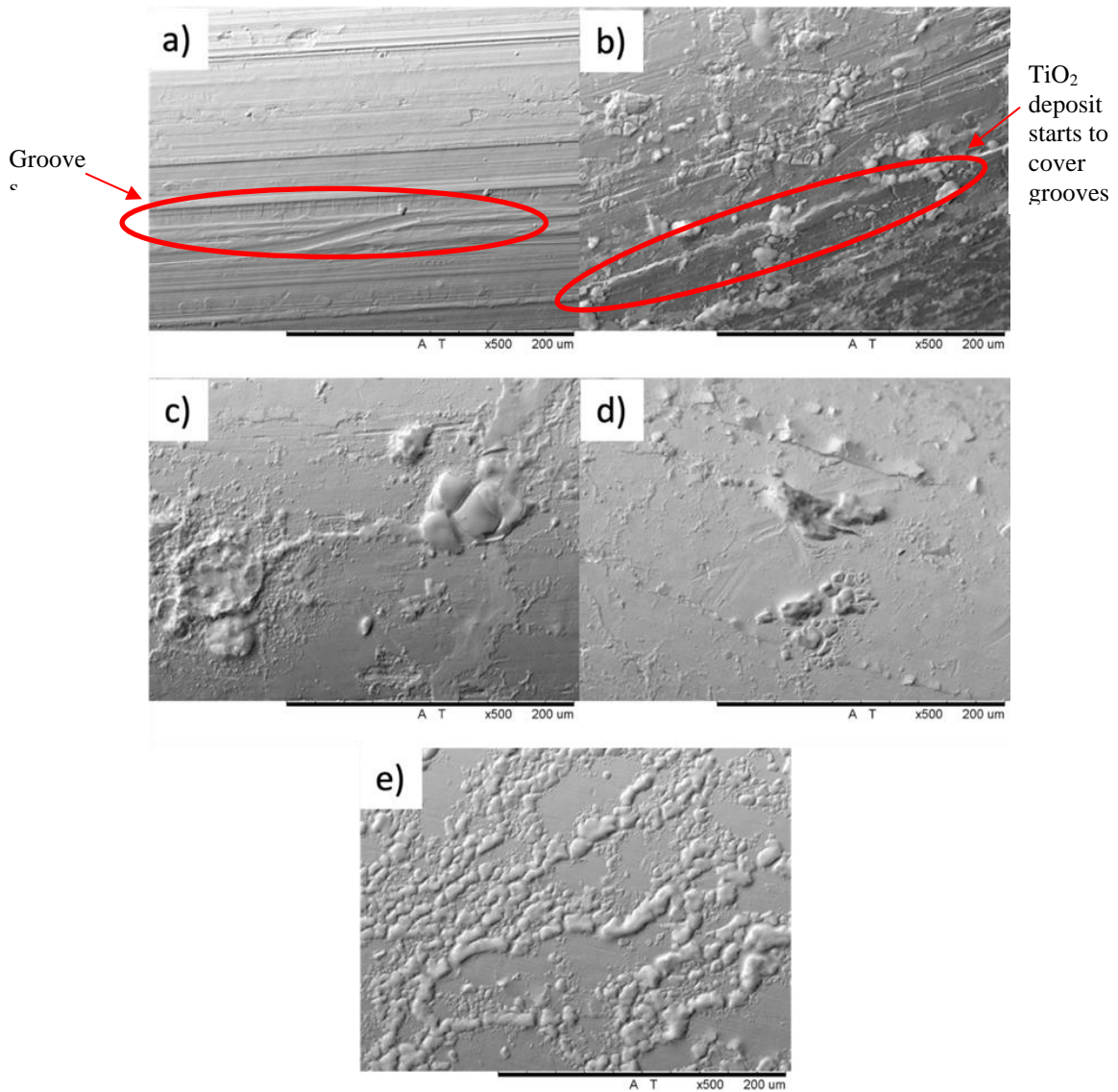
Figure 4. The surface morphology of TiO$_2$ deposited on kanthal coils using 60 W applied power for (a) 0 (bare Kanthal wire), (b) 15, (c) 30, (d) 45 and (e) 60 min at magnification of 500X.
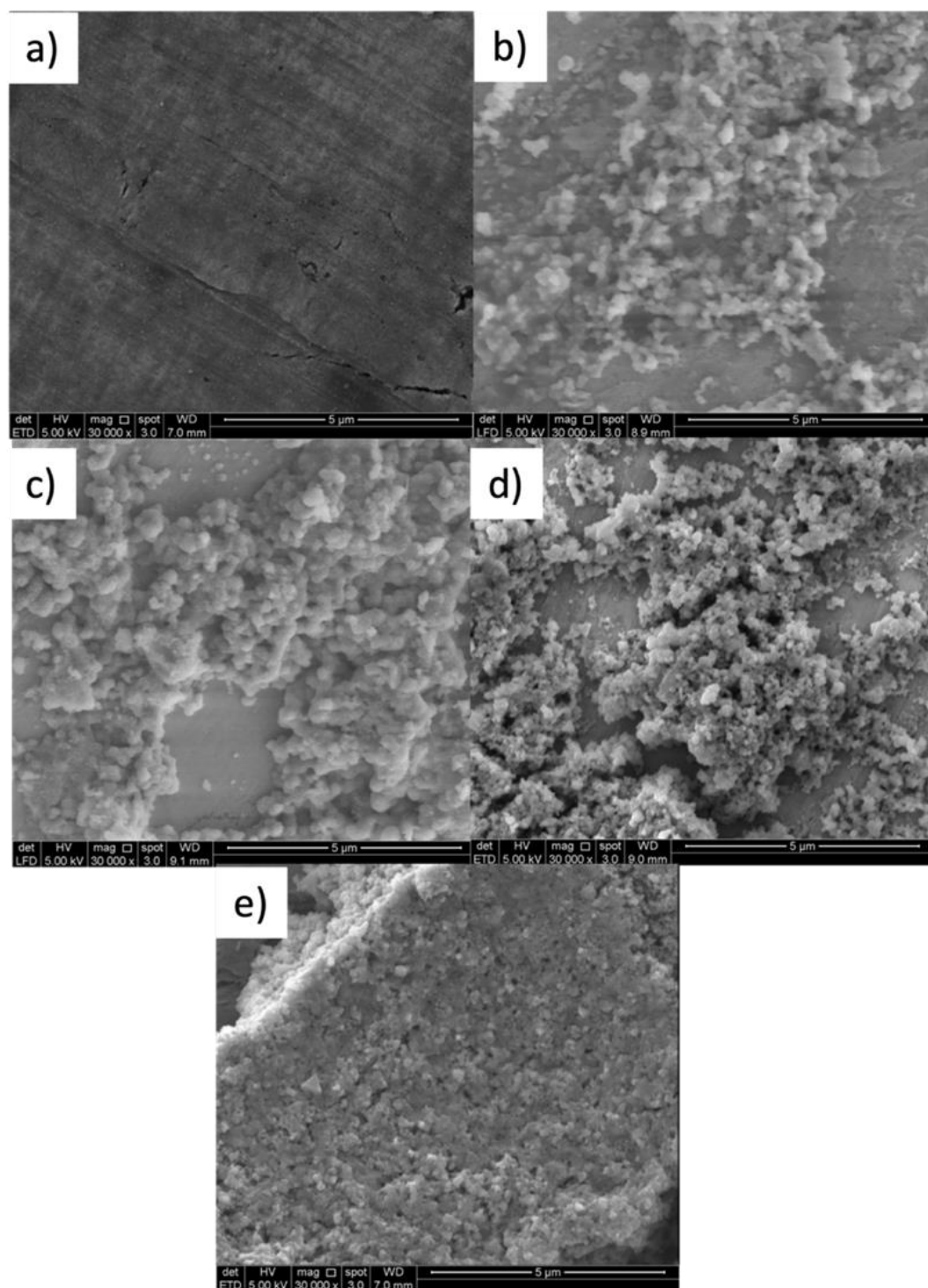
Figure 5. The surface morphology of TiO$_2$ deposited on kanthal coils using 60 W applied power for (a) 0 (bare Kanthal wire), (b) 15, (c) 30, (d) 45 and (e) 60 min at magnification of 30kX.

Table 2 displays the size of TiO$_2$ particles (n = 30) deposited on the surface Kanthal wires at different heating durations that analyzed using Image J. As shown in **Figure 6**, there is not much different in the particles size regardless the synthesis duration. A one-way ANOVA is performed ($\alpha = 0.05$), verifying that is no significant different amongst the size of TiO$_2$ particles. These results suggest that pro-long heating duration produced more TiO$_2$ particles that deposited on the surface of Kanthal wires, but with no effect on the particles' size. This is because pro-long the synthesis duration would result in more uniform heating of precursor solution particularly at the

adjacent of kanthal coil. As a result, more nucleation occurred on the surface of kanthal coil, producing more TiO_2 particles. Similar result was observed for TiO_2 particles that synthesized by hydrothermal method. The TiO_2 particles tended to be agglomerated at a longer synthesis duration, forming thick TiO_2 layer.

Table 2 The size of TiO_2 nanoparticles deposited on kanthal coils synthesized at different heating duration (n = 30)

Synthesis duration (min)	Size of TiO_2 particles (nm)	
	Mean	Standard Deviation
0	-	-
15	167.36	15.37
30	146.66	18.02
45	158.99	21.25
60	155.97	19.68
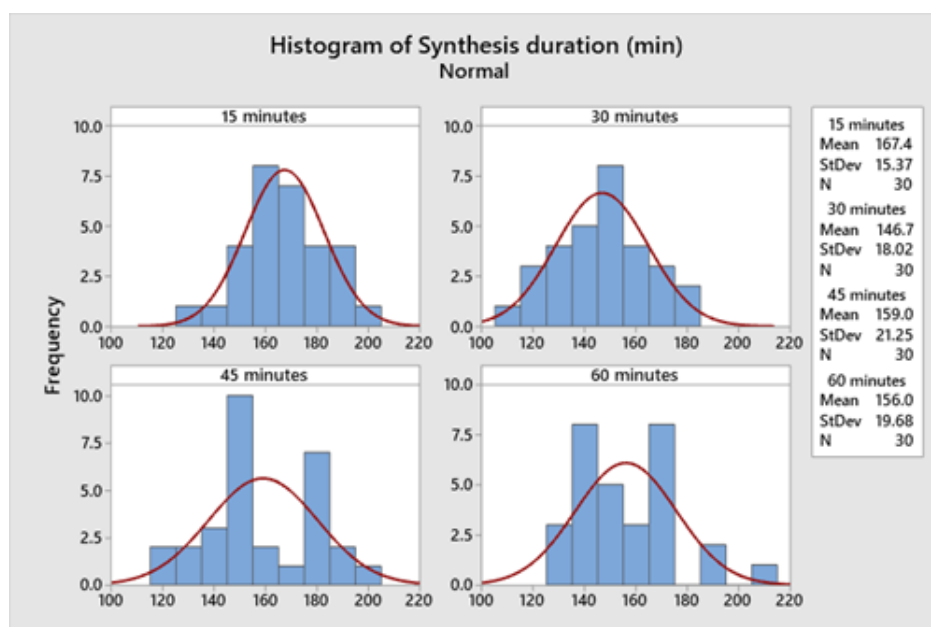
Figure 6. The size distribution of TiO_2 particles deposited on kanthal coils using 60 W for (a) 15, (b) 30, (c) 45 and (d) 60 min

The TiO_2 particles deposited on kanthal coils at 15 min condition were further analyzed using TEM and HRTEM. As shown in **Figure 7 (a),** the TiO_2 nanostructures consisted of nanorods, surrounded by irregular nanoparticles. **Figure 7 (b)** and **Figure 7 (c)** show morphology of TiO_2 of nanorods taken at higher magnification from the region as highlighted in red circles. **Figure 7 (d)** depicts the lattice spacing of anatase (101) and brookite (121) correspond to 0.352 nm and 0.292 nm respectively. This finding is aligned with the XRD analysis in **Figure 3**.

Figure 8 shows the EDX spectrum of TiO_2 particles deposited on kanthal coil at 15 min by DH technique. The presence of Ti and O elements verified that the deposit was TiO_2 particles. The C element could be due to contamination from environment during sample preparation process for EDX measurement. The origin of Cl element was from the HCl acid which used in the synthesis process. The sharp peak at 0 keV is the noise peak from the detector.
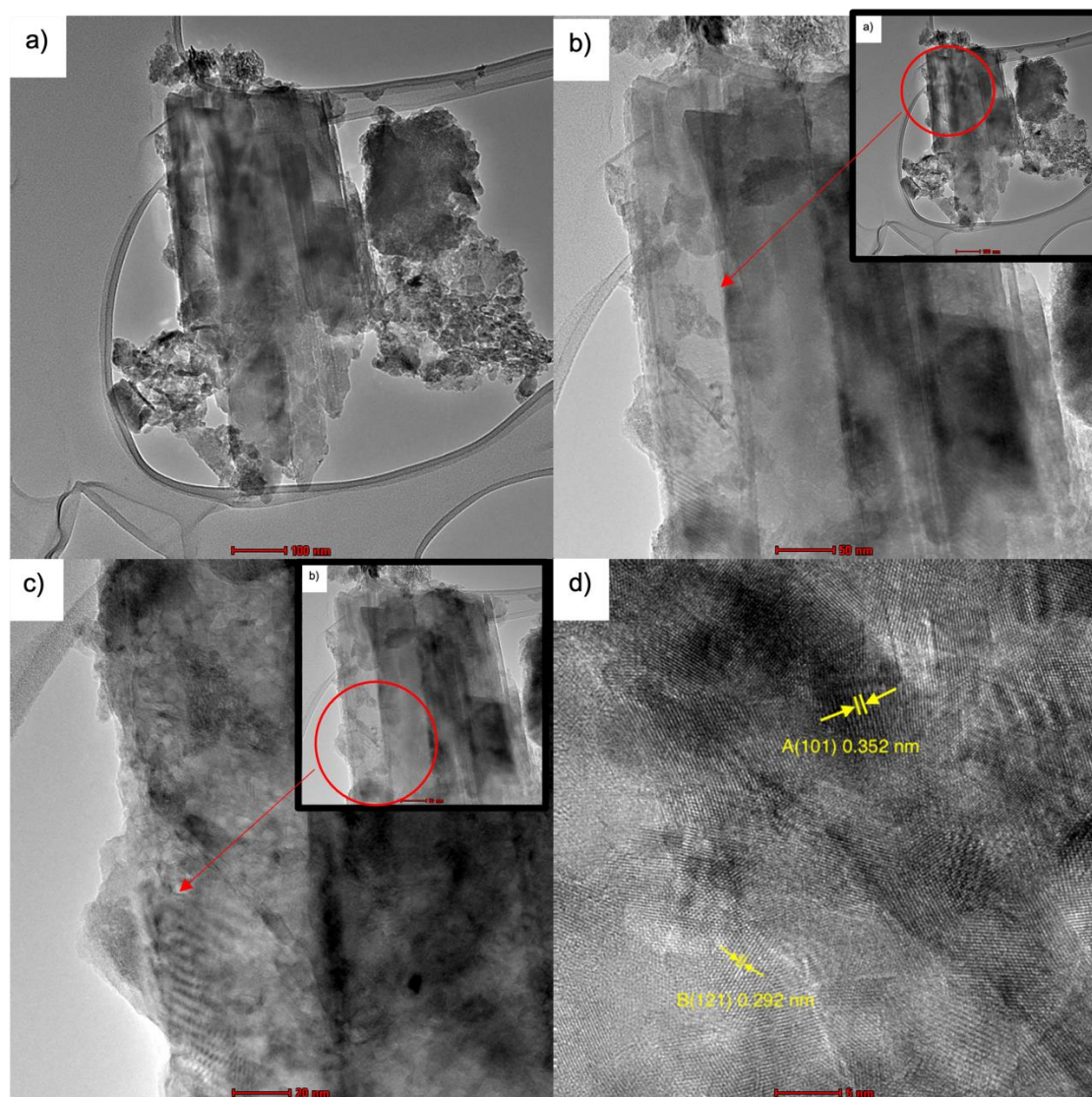
Figure 7. TEM images of TiO₂ particles deposited on kanthal coil captured at the magnification of (a) 43kX, (b) 97kX, (c) 195kX; (d) HRTEM image shows the presence of anatase phase and brookite phase TiO₂ (15 min at 60 W).
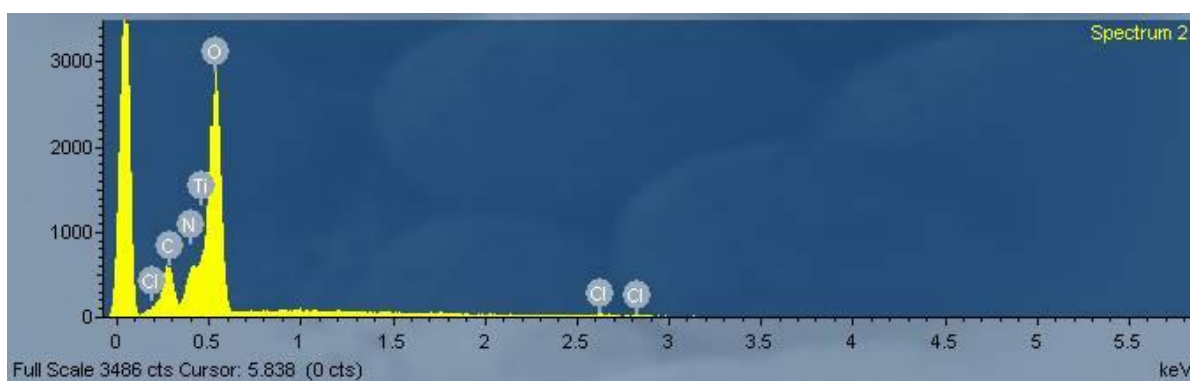
Figure 8. The EDX analysis of TiO₂ particles deposited on kanthal coil (15 min at 60 W).

3.3 Growth mechanism of TiO₂ particles on kanthal coil by DH technique

The formation of TiO_2 particles on the kanthal coils could be explained by an acid-catalyzed step of TTIP solution. The process involved 2 reactions, i.e., (i) hydrolysis, and (ii) polycondensation to form TiO_2 particles. Firstly, the TTIP solution was added dropwise into acid solution. The TTIP solution underwent hydrolysis process when added in water to form titanium hydroxide precipitates ($Ti(OH)_4$) and ROH product as shown in Eq. (5). Then, the titanium hydroxide precipitates would undergo polycondensation to form the complex three-dimensional network of titanium nuclei. Polycondensation could be produced between two hydroxyl groups (oxolation) or between an un-hydroxylated alkoxide group and a hydroxyl group (alcoxolation) as shown in Equation (6) and (7).

Step (i) Hydrolysis:

$$Ti(OC_3H_7)_4 + H_2O \rightarrow Ti(OH)_4 + 4(C_3H_7)(OH) \tag{5}$$

Step (ii) Condensation:

$$Ti(OH)_4 + Ti(OH)_4 \rightarrow 2TiO_2 + 4H_2O \text{ (Oxolation)} \tag{6}$$

$$Ti(OH)_4 + Ti(OC_3H_7)_4 \rightarrow 2TiO_2 + 4(C_3H_7)(OH) \text{ (Alcoxolation)} \tag{7}$$
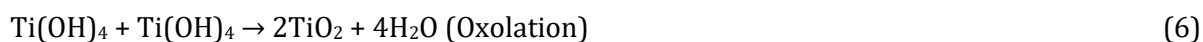
The DH process triggered the above chemical reactions by supplying sufficient heat to overcome their activation energy. The highly resistive kanthal coil was heated when electrical power supply was switched on. The heat produced from the wire coil would result in primary nucleation and crystallization of TiO_2 particles on the surface of kanthal coil.

The formation of anatase and brookite phases of TiO_2 could be explained by the formation mechanism of TiO_2 from its precursor solution, i.e., TTIP solution (titanium alkoxides). The formation of TiO_2 particles involved of hydrolysis of 4-coordinated $[Ti(OR)_4]$ in the water. The titanium ions accepted the oxygen lone pairs through the vacant *d*-orbitals forming $[Ti(H_2O)_6]^{4+}$ ions and consequently increased its coordination. These species underwent partial deprotonations and formed the octahedral monomers (TiO_6^{2-}). In the subsequent condensation step, the anatase and brookite phases would be grown from the TiO_6^{2-} octahedra. The anatase TiO_2 shares two sets of two adjacent edges to form zigzag chains linked to one another; whereas brookite phase TiO_2 shared three edges of TiO_6^{2-} octahedra units [23].

3.4   *Methylene blue removal by TiO₂ particles deposited on kanthal coils using different synthesis duration.*

The MB solution was degraded by the TiO_2 particles deposited on kanthal coils prepared using various heating durations. The dye removal performance by the TiO_2 particles was studied under UV light ($\lambda = 254$ nm) as the band gap of TiO_2 is larger than 3 eV which makes TiO_2 only absorbs and activates under the irradiation of UV light [24]. **Figure 9** shows the UV-Vis absorbance spectra of MB solution degraded by TiO_2 particles on kanthal coils prepared using different synthesis duration. The decrease in absorption intensities is observed in all samples, suggesting that the MB was degraded by the TiO_2 particles under UV light irradiation.
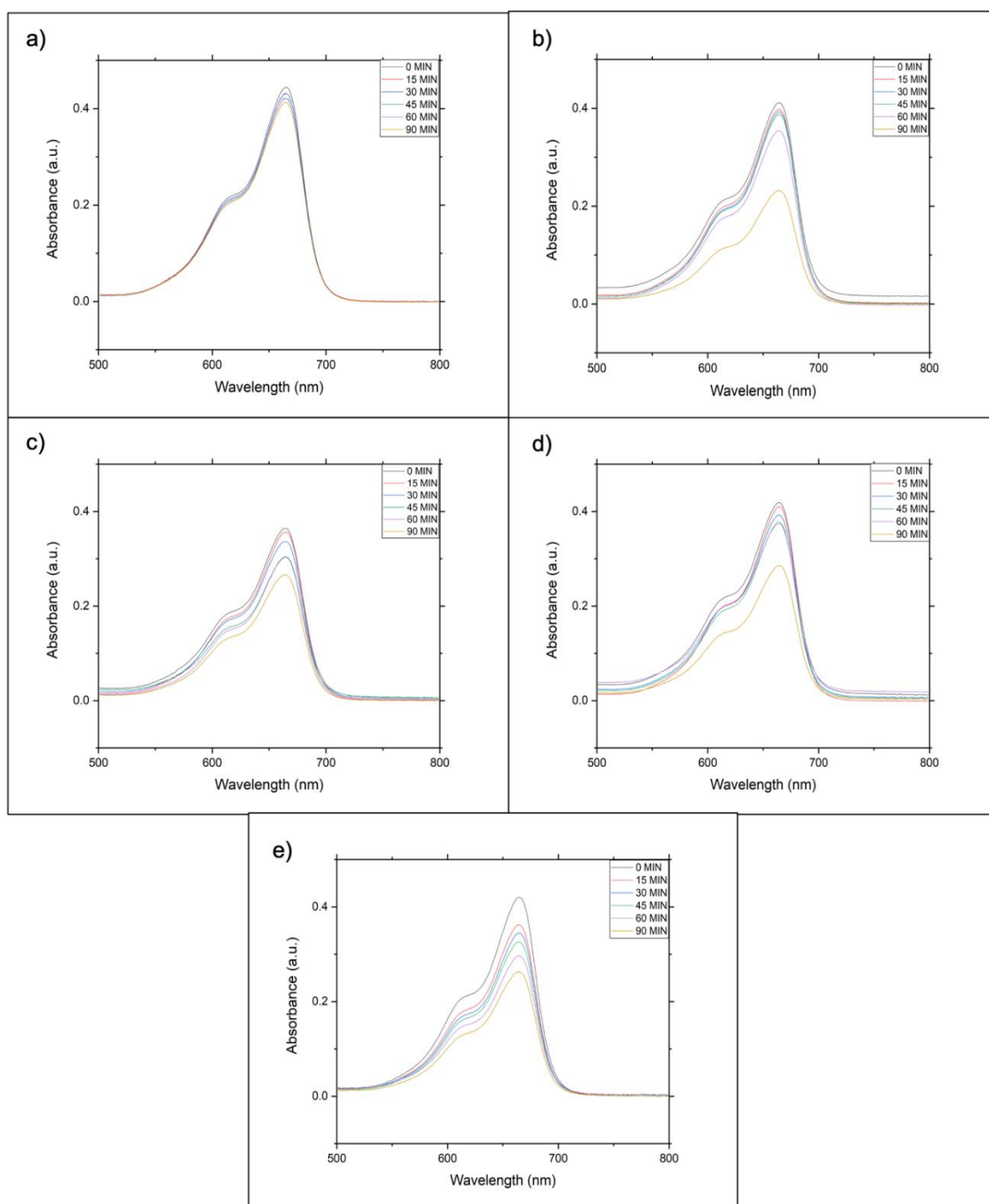
Figure 9. UV-Vis absorbance spectra of MB solution degraded by TiO_2 particles on Kanthal wires prepared at (a) 0 (bare Kanthal wire), (b) 15, (c) 30, (d) 45 and (e) 60 min

The photodegradation efficiency of each sample at each time interval was calculated using Equation 1. **Table 3** summarizes the photodegradation efficiencies of samples produced at different heating durations. The photodegradation efficiencies of TiO_2 particles deposited on kanthal coils as a function of UV irradiation time which is shown in **Figure 10(a)**. The photodegradation efficiency of photocatalyst increased when the irradiation time of UV light increased from 0 to 90 min. This was due to the interaction of more dye molecules with the surface of photocatalyst, allowing reactive species to breakdown the dye molecules into smaller fragments [25]. **Figure 10(b)** shows the photodegradation efficiency at 90 minutes of UV irradiation. The bare kanthal coil (0 min) shows the lowest photodegradation efficiency, i.e. at 7.6 %. The result suggests that the degradation of MB by UV light was low even after 90 min. The

degradation of MB dye without catalyst was used as a baseline. The best photocatalytic performance was TiO_2 particles deposited on kanthal coils prepared at 15 min, achieving of 43.7% photodegradation efficiency. The 15 min sample shows the least agglomeration based on the FESEM result. Moreover, it has the highest photocatalytic activity due to the presence of mixed phases (anatase/brookite) as electrons transfer from brookite conduction band to anatase conduction band resulting in efficient electron-hole separation and minimize the recombination of positive holes and electrons.

Table 3 Photodegradation efficiency of samples at different synthesis duration

Synthesis duration \ Irradiation time	Photodegradation Efficiency (%)					
	0 min	15 mins	30 mins	45 mins	60 mins	90 mins
0 (baseline)	0.0	3.1	3.1	5.3	5.6	7.6
15 mins	0.0	3.6	4.6	5.9	14.2	43.7
30 mins	0.0	2.1	7.6	16.3	16.9	27.2
45 mins	0.0	2.0	6.4	10.1	10.7	29.6
60 mins	0.0	14.1	18.2	22.9	29.6	37.8
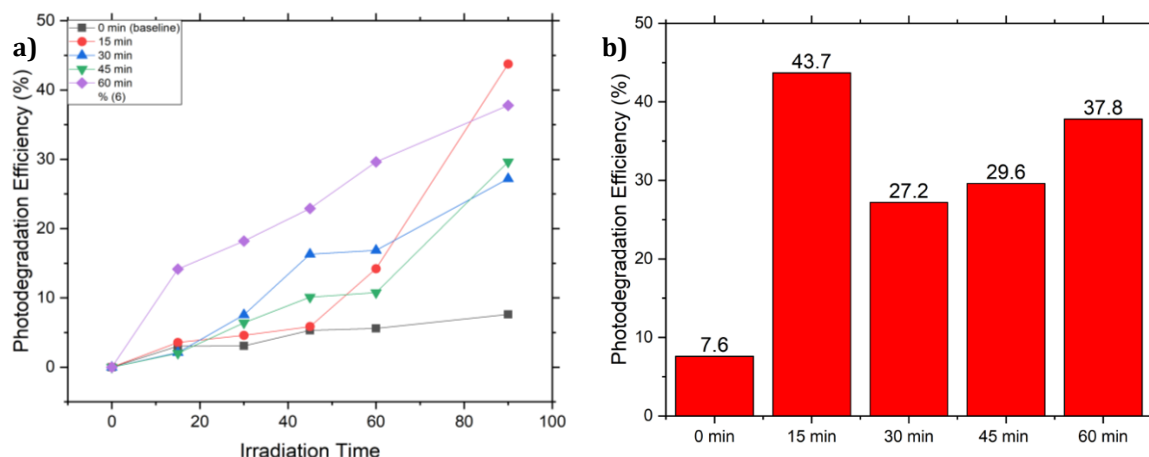
Figure 10. Photodegradation efficiency of MB dye degraded by TiO_2 particles synthesized using different durations (a) as a function of UV light irradiation time, and (b) at 90 min of UV light irradiation

The kinetic reaction of MB dye by TiO_2 particles grown on kanthal coils synthesized at different heating durations was investigated by plotting the graphs in pseudo-zero-order, pseudo-first-order, and pseudo-second-order as illustrated in **Figure 11 (a)–(c)**. Regression analysis was performed to obtain the kinetic plots. **Table 4** shows the rate constants and correlation coefficient (R^2) for all fittings. Generally, the average R^2 values of all fittings for pseudo-zero-order has the highest R^2 which is 0.938 if compared to pseudo-first-order (0.926) and pseudo-second-

order (0.911). This means the degradation of MB dye by TiO_2 particles grown on kanthal coils synthesized at different heating duration followed the pseudo-zero-order kinetic model. Pseudo-zero-order kinetic model means the degradation of MB dye by TiO_2 particles grown on kanthal coils synthesized at different heating duration did not depend on the concentration of the MB solution. This could be explained by the Langmuir-Hinshelwood (L-H) model as shown in Equation 8, where K and k are the thermodynamic adsorption constant and photodegradation rate constant, respectively. When the concentration of dye was high, the surface of photocatalyst would be fully covered, leading to the approximation of (1 + KC) to KC. Therefore, a pseudo-zero-order was observed for saturation coverage on the surface of the photocatalyst, since the photodegradation rate was independent of the change in dye concentration, as shown in Equation 9 [26].

$$-\frac{dC}{dt} = \frac{kKC}{1+KC},$$ (8)

$$-\frac{dC}{dt} = k$$ (9)
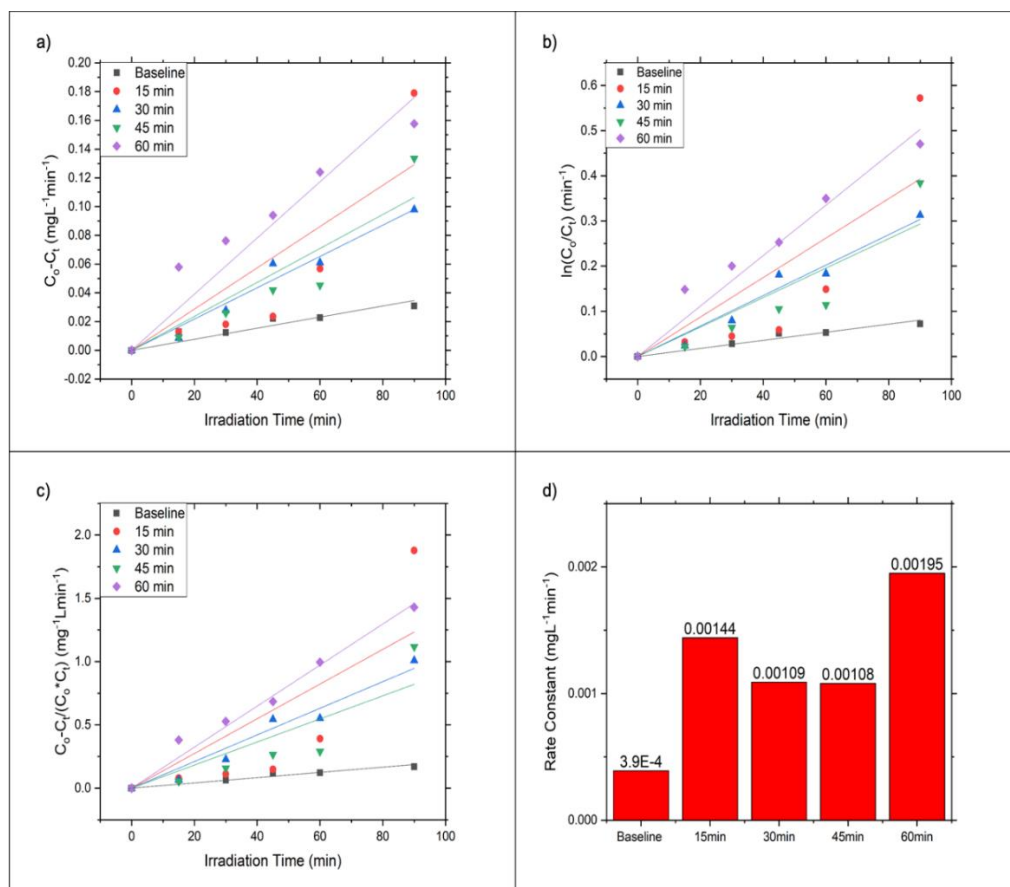
Figure 11. Kinetic plots of (a) Pseudo-zero-order, (b) Pseudo-first-order, (c) Pseudo-second-order; and (d) rate constants for photodegradation of MB dye by TiO_2 particles grown on kanthal coils synthesized at different heating durations.

Table 4 Kinetic parameters for the degradation of MB dye by TiO_2 particles grown on kanthal coils synthesized at different synthesis durations

Order of reaction	Parameters	Unit	Synthesis Duration (min)				
			0 (baseline)	15	30	45	60
Pseudo zero order	K_0	$mgL^{-1}min^{-1}$	0.00039	0.00144	0.00109	0.00108	0.00195
	R^2	-	0.96125	0.84247	0.98718	0.92468	0.97348
Pseudo first order	K_1	min^{-1}	0.0009	0.00437	0.00337	0.00326	0.00559
	R^2	-	0.91562	0.79695	0.78373	0.89578	0.98614
Pseudo second order	K_2	$mg^{-1}Lmin^{-1}$	0.00208	0.01371	0.01052	0.00912	0.01621
	R^2	-	0.96557	0.75079	0.98146	0.86303	0.99388

4. CONCLUSION

TiO_2 particles was successfully deposited on kanthal coils by DH technique. By varying heating duration, it was found that the sample produced at 15 min of synthesis duration and 60 W has the highest photodegradation efficiency (43.7%) on the degradation of MB dye under UV light. The crystal phase of the sample contained mixture of anatase (82.7%) and brookite (17.3%). The TiO_2 particles has a size 167.36 ±15.37 nm and the surface coverage of TiO_2 particles on kanthal coils was good with minimum agglomeration. Besides, regression analysis was carried out and the results shows that the degradation of MB dye by TiO_2 particles produced from DH technique followed the pseudo-zero-order kinetic model. The DH technique demonstrates its capability to deposit TiO_2 particles on kanthal coils in short synthesis duration (15 min) with very low electrical power consumption (60 W).

ACKNOWLEDGEMENTS

REFERENCES

[1] G. Upendar, G. Biswas, K. Adhikari, and S. Dutta, "Adsorptive removal of methylene blue dye from simulated wastewater using shale: Experiment and modelling," *Journal of the Indian Chemical Society,* vol. 94, pp. 971-982, 2017.

[2] A. Hussain and M. Asi, "Pesticides as water pollutants," in *Groundwater for Sustainable Development*: CRC Press, pp. 119-126, 2008.

[3] T. Seema, H. Tiwari, and I. Tripathi, "Effects of Lead on Environment " *International Journal of Emerging Research in Management &Technology,* vol. 2, no. 6, pp. 2278-9359, 2013.

[4] E. Shaji, M. Santosh, K. Sarath, P. Prakash, V. Deepchand, and B. Divya, "Arsenic contamination of groundwater: A global synopsis with focus on the Indian Peninsula," *Geoscience frontiers,* vol. 12, no. 3, p. 101079, 2021.

[5] X. Cui *et al.*, "Polychlorinated biphenyls in the drinking water source of the Yangtze River: characteristics and risk assessment," *Environmental Sciences Europe,* vol. 32, no. 1, pp. 1-9, 2020.

[6] Y. Zhang *et al.*, "Pollution of polycyclic aromatic hydrocarbons (PAHs) in drinking water of China: Composition, distribution and influencing factors," *Ecotoxicology and environmental safety,* vol. 177, pp. 108-116, 2019.

[7] M. Munir *et al.*, "Effective adsorptive removal of methylene blue from water by didodecyldimethylammonium bromide-modified Brown clay," *ACS omega,* vol. 5, no. 27, pp. 16711-16721, 2020.

[8]   S. Dutta, B. Gupta, S. K. Srivastava, and A. K. Gupta, "Recent advances on the removal of dyes from wastewater using various adsorbents: A critical review," *Materials Advances,* 2021.

[9]   F. Sadeghfar, M. Ghaedi, and Z. Zalipour, "Chapter 4 - Advanced oxidation," in *Interface Science and Technology*, vol. 32, M. Ghaedi Ed.: Elsevier, pp. 225-324, 2021.

[10]   R. Ameta, M. S. Solanki, S. Benjamin, and S. C. Ameta, "Chapter 6 - Photocatalysis," in *Advanced Oxidation Processes for Waste Water Treatment*, S. C. Ameta and R. Ameta Eds.: Academic Press, pp. 135-175, 2018.

[11]   D. Ghime and P. Ghosh, "Advanced oxidation processes: a powerful treatment option for the removal of recalcitrant organic compounds," in *Advanced Oxidation Processes-Applications, Trends, and Prospects*: IntechOpen, 2020.

[12]   A. ul Haq, M. Saeed, S. G. Khan, and M. Ibrahim, "Photocatalytic Applications of Titanium Dioxide (TiO 2)," in *Titanium Dioxide-Advances and Applications*: IntechOpen, 2021.

[13]   K. C. Sun, M. B. Qadir, and S. H. Jeong, "Hydrothermal synthesis of TiO 2 nanotubes and their application as an over-layer for dye-sensitized solar cells," *RSC advances,* vol. 4, no. 44, pp. 23223-23230, 2014.

[14]   L.-H. Yang, T.-Y. Yang, K.-y. Wang, T.-Y. Su, D.-C. Wu, and Y.-L. Cheuh, "Three-dimensional CuO/TiO2 hybrid nanorod arrays prepared by electrodeposition in AAO membranes as an excellent Fenton-like photocatalyst for dye degradation," *Nanoscale research letters,* vol. 15, no. 1, pp. 1-12, 2020.

[15]   C. B. Marien, C. Marchal, A. Koch, D. Robert, and P. Drogui, "Sol-gel synthesis of TiO2 nanoparticles: effect of Pluronic P123 on particle's morphology and photocatalytic degradation of paraquat," *Environmental Science and Pollution Research,* vol. 24, no. 14, pp. 12582-12588, 2017.

[16]   D. Bhattacharyya, Y. R. Smith, S. K. Mohanty, and M. Misra, "Titania nanotube array sensor for electrochemical detection of four predominate tuberculosis volatile biomarkers," *Journal of the Electrochemical Society,* vol. 163, no. 6, p. B206, 2016.

[17]   A. May-Masnou, L. Soler, M. Torras, P. Salles, J. Llorca, and A. Roig, "Fast and simple microwave synthesis of TiO2/Au nanoparticles for gas-phase photocatalytic hydrogen generation," *Frontiers in chemistry,* vol. 6, p. 110, 2018.

[18]   Q. Zhang and C. Li, "Pure anatase phase titanium dioxide films prepared by mist chemical vapor deposition," *Nanomaterials,* vol. 8, no. 10, p. 827, 2018.

[19]   S.-L. Chiam, Q.-Y. Soo, S.-Y. Pung, and M. Ahmadipour, "Polycrystalline TiO2 particles synthesized via one-step rapid heating method as electrons transfer intermediate for Rhodamine B removal," *Materials Chemistry and Physics,* vol. 257, p. 123784, 2021/01/01/ 2021.

[20]   Z. Yanqing, S. Erwei, C. Zhizhan, L. Wenjun, and H. Xingfang, "Influence of solution concentration on the hydrothermal preparation of titania crystallites," *Journal of materials Chemistry,* vol. 11, no. 5, pp. 1547-1551, 2001.

[21]   R. L. Penn and J. F. Banfield, "Oriented attachment and growth, twinning, polytypism, and formation of metastable phases: Insights from nanocrystalline TiO2," *American Mineralogist,* vol. 83, no. 9-10, pp. 1077-1082, 1998.

[22]   M. M. Ahmad, S. Mushtaq, H. S. Al Qahtani, A. Sedky, and M. W. Alam, "Investigation of TiO2 Nanoparticles Synthesized by Sol-Gel Method for Effectual Photodegradation, Oxidation and Reduction Reaction," *Crystals,* vol. 11, no. 12, p. 1456, 2021.

[23]   D. M. EL-Mekkawi, A. A. LAbIb, H. A. Mousa, H. R. Galal, and W. A. Mohamed, "Preparation and characterization of nano titanium dioxide photocatalysts via sol gel method over narrow ranges of varying parameters," *Oriental journal of chemistry,* vol. 33, no. 1, p. 41, 2017.

[24]   T. Luttrell, S. Halpegamage, J. Tao, A. Kramer, E. Sutter, and M. Batzill, "Why is anatase a better photocatalyst than rutile?-Model studies on epitaxial TiO2 films," *Scientific reports,* vol. 4, no. 1, pp. 1-8, 2014.

[25]   A. Kumar and G. Pandey, "The photocatalytic degradation of methyl green in presence of visible light with photoactive Ni0. 10: La0. 05: TiO2 nanocomposites," *IOSR Journal of Applied Chemistry,* vol. 10, no. 9, pp. 31-44, 2017.

[26]   Y.-H. Chiu, T.-F. M. Chang, C.-Y. Chen, M. Sone, and Y.-J. Hsu, "Mechanistic insights into photodegradation of organic dyes using heterostructure photocatalysts," *Catalysts,* vol. 9, no. 5, p. 430, 2019.